Theoretical evaluation of hydrogen storage capacity in pure carbon nanostructures

Ju Li
Department of Materials Science and Engineering, Ohio State University, Columbus, Ohio 43210

Terumi Furuta, Hajime Goto, Toshiyuki Ohashi, and Yoshiya Fujiwara
Honda R&D Co., Ltd., Wako Research Center, 1-4-1 Chuo Wako, Saitama 351-0193, Japan

Sidney Yip[a)]
Department of Nuclear Engineering and Department of Materials Science and Engineering, Massachusetts Institute of Technology, Cambridge, Massachusetts 02139

(Received 16 December 2002; accepted 24 April 2003)

Carbon nanotubes have been proposed as promising hydrogen storage materials for the automotive industry. By theoretical analyses and total-energy density functional theory calculations, we show that contribution from physisorption in nanotubes, though significant at liquid nitrogen temperature, should be negligible at room temperature; contribution from chemisorption has a theoretical upper limit of 7.7 wt %, but could be difficult to utilize in practice due to slow kinetics. The metallicity of carbon nanotube is lost at full hydrogen coverage, and we find strong covalent C–H bonding that would slow down the H_2 recombination kinetics during desorption. When compared to other pure carbon nanostructures, we find no rational reason yet why carbon nanotubes should be superior in either binding energies or adsorption/desorption kinetics. © *2003 American Institute of Physics.* [DOI: 10.1063/1.1582831]

I. INTRODUCTION

Fuel cell electric vehicles require efficient storage and extraction of H_2 with the following characteristics: (a) high storage capacity (usable H_2 weight$>6\%$ of the storage system weight), (b) near room temperature and/or ambient pressure operation, (c) quick uptake/extraction, in a matter of seconds (the targeted refuel time is <10 min), (d) stability and reusability. Some of the technologies under development are: high pressure tank, metal hydride, and activated carbon. We focus on pure carbon materials in this paper.

Since the report of high-capacity storage of hydrogen in single-walled carbon nanotubes (SWNTs),[1] there have been a number of experimental results of near room temperature hydrogen storage in graphitic nanofibers and alkali-doped and sonicated carbon nanotubes[2–4] which potentially can fulfill the above-mentioned requirements. However to date none of the above-mentioned experiments have been reproduced by independent groups.[5,6] As there may be many hard-to-control factors in these experiments, it is difficult to determine why two experiments give different results.[7] What we do instead in this paper is to start with some simple theory and calculations, and then relate to the experiments. There have been a number of calculations about either physisorption[8–11] or chemisorption,[12–14] but none have yet given a complete picture leading to practical conclusions.

II. SIMPLIFIED ANALYSIS

The difference in chemical potential of hydrogen in free and adsorbed states $\Delta\mu=\Delta h-T\Delta s$ controls the direction of adsorption/desorption, where Δh is the change in specific enthalpy and Δs is the change in specific entropy of hydrogen. One H_2 molecule in gas state at $T=298$ K and 1 atmosphere pressure has about $15.6k_B$ entropy.[15] There is no accurate estimate of the entropy of hydrogen in adsorbed state because up to now there is no agreement on what that state is, but it is probably safe to assume that it is much less than that of the gas state. Therefore in order for near room temperature adsorption/desorption to occur, Δh should be about $10-15\ k_BT$ per molecule, which is equivalent to about 0.15 eV binding enthalpy per H atom. For automotive applications, Δh also should be a weak function of the coverage X, because we expect hydrogen to stay absorbed to almost saturation in the hottest weather ($T=330$ K), but desorbed to almost zero X at no more than $T=400$ K, which is the upper temperature limit provided by the fuel-cell heat-recycling system. So we expect $\Delta h(X)$ to be from 0.15 eV per H atom to 0.2 eV per H atom, for instance, when X varies from almost saturation to almost zero.

There are two ways hydrogen can be absorbed: physisorption, where H_2 keeps its molecular identity, or chemisorption, where H_2 molecules dissociate and hydrogen is stored in atomic form. In the former, the binding energy needs to be 0.3–0.4 eV per H_2. In a density functional theory (DFT) calculation,[16] the binding energy of a H_2 molecule onto a flat graphene sheet is computed to be 0.07–0.086 eV depending on the site (rotational degrees of freedom have been optimized), with an equilibrium distance of 2.68–2.91 Å. Assuming this level of sheet-H_2 binding energy can be carried over to the nanotube, it appears there will not be sufficient binding between a H_2 molecule and an isolated SWNT, or if the H_2 molecule is in the interstice be-

a)Electronic mail: syip@mit.edu

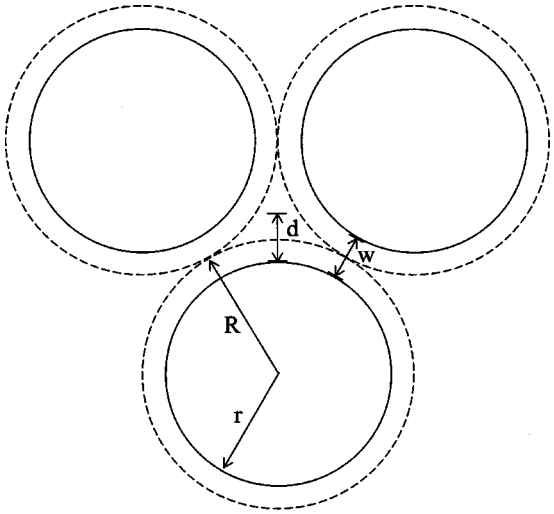

FIG. 1. Physisorption of H_2 molecule in triple junction of SWNT bundle.

tween two SWNTs, by quite a large margin (the binding between H_2 molecules is very weak as the boiling point of H_2 is 20.28 K). In the case of triple junction configuration (see Fig. 1) which occurs in SWNT bundles, the best possible binding energy (3×0.086 eV) matches roughly with the requirement (0.3–0.4 eV) within error of calculation, but there are additional geometrical considerations. (a) The distance between the junction center and a tube wall is $d=(2/\sqrt{3}-1)R+w/2\approx0.15R+w/2$, where w is the separation between two nanotube walls, and $R=r+w/2$, where r is the radius of the nanotube. If we set $w=3.4$ Å, the graphite interlayer spacing that has been confirmed experimentally to match closely with wall spacing in carbon nanotube bundles, and $r=5.4$ Å, the radius of (8,8) SWNT, we find $d=2.80$ Å, which matches the optimal H_2-wall separation of 2.68–2.91 Å. Nanotubes with radius much greater or smaller than that of (8,8), will be unable to take advantage of the triple junction. (b) The triple junctions are too scarce. Consider the following: if one carbon atom corresponds to one adsorbed H atom, the storage capacity is $1/(1+12)\approx7.7$ wt %. Because each triple junction is shared by three SWNTs, one SWNT ''owns'' two junctions. A (5,5) SWNT has 20 carbon atoms per unit cell that has 2.5 Å repeat distance in the longitudinal direction. Based on a recent coupled-cluster theory calculation[17] of H_2-H_2 interactions, one sees that once the distance between two H_2 molecules is smaller than 2.5 Å, the repulsion between them is so strong that the wall–H_2 binding becomes relatively insignificant. Therefore one H_2 molecule can barely fit into one junction per unit cell, which corresponds to $2\times2/20\times7.7$ wt % $=1.5$ wt % upper limit under this highly idealized condition.

Without doing a direct molecular dynamics or Monte Carlo calculation, the above-given analysis agrees qualitatively with the results of many detailed physisorption simulations. Wang *et al.*[10] used the Crowell–Brown van der Waals potential[18] for graphene sheet–H_2 interactions and grand canonical Monte Carlo simulation, and concluded that it is not possible to achieve the U.S. Department of Energy target storage capacity of 6.5 wt % at ambient temperature even if the wall–H_2 interactions are increased threefold. Williams *et al.*[11] performed simulations using a different C–H_2 potential[19] deduced from scattering experiments; their results show that the net storage capacity is 5.5 wt % at $T=77$ K and 100 atm pressure in a 7-SWNT bundle, but drops to less than 1 wt % at $T=300$ K and the same pressure. Based on molecular dynamics simulation results, Maruyama[20] concluded that at room temperature normal physisorption mechanism cannot explain the hydrogen storage capacity of SWNTs of more than 1 wt %. Experimentally, Ye *et al.*[21] have measured hydrogen storage capacity exceeding 8 wt % at $T=80$ K and $P=120$ atm, but some of the same researchers found[22] that the storage capacity is less than or about 0.1 wt % at room temperature in graphitic nanofibers (we note that SWNTs and graphitic nanofibers are different nanostructures, but the same estimate above based on graphene sheet–H_2 interaction should be applicable to a large extent to both). Williams *et al.*[23] measured the Raman spectra of H_2 adsorbed on SWNT and C_{60} at $T=85$ K and calculated frequency shifts compared to the results for H_2 adsorbed on graphite, and concluded these shifts are small and are therefore inconsistent with charge transfer; a new H_2-surface potential was developed based on the new results which is not drastically different from the previous ones.[18,19] In summary, the majority of evidence up to now suggests that it may be possible to store a significant amount of H_2 (more than 5 wt %) by physisorption in SWNTs at cryogenic (liquid nitrogen) temperatures, but that contribution should be almost negligible (less than 1 wt %) near $T=300$ K, a conclusion that is consistent with our simple analysis without going into the detailed calculations.

In the present analysis, a critical hypothesis is that the binding energy of a H_2 molecule to the SWNT wall is close enough in magnitude to the binding energy of a H_2 molecule to a flat graphene sheet or graphite surface. In other words, there are no abnormal interactions besides the ordinarily small and pair-additive van der Waals interactions. One recent density functional theory calculation suggested otherwise.[24] Cheng *et al.* performed finite-temperature *ab initio* molecular dynamics simulation of H_2 molecules in a trigonal lattice of (9,9) SWNTs using the Vienna Ab-Initio Simulation Package (VASP).[25] By evaluating the time-averaged total energies before and after the H_2 molecules were introduced, the authors extracted Δh explicitly, which turned out to be 7.51 kcal/mol or 0.33 eV/H_2 for endohedral (inside SWNT) configuration, and 6.75 kcal/mol or 0.29 eV/H_2 for exohedral (outside SWNT) configuration, at $T=300$ K. These numbers are far outside of the range of our estimate (0.05–0.1 eV/H_2), and if true, would call into question our conclusions with regard to physisorption in SWNT. Because the method of Cheng *et al.* did not resort to an empirical potential, it was free from the unverified hypothesis on which all previous simulations[8–11,20] are based.

This is such an important issue to check out that we have performed our own calculations using the same VASP program. But instead of carrying out tens of thousands of molecular dynamics steps, we apply our limited computer resources on doing static relaxations, but at an accuracy level (energy cutoff, Brillouin zone integration, etc.) that should be significantly higher than what had been used.[24] We arrived at

a conclusion that is very different from Ref. 24, so we believe the results of Refs. 8–11, and 20 are still largely correct. Section III will be devoted to these calculations.

III. DENSITY FUNCTIONAL THEORY CALCULATION OF PHYSISORPTION ENERGIES

The results of Cheng *et al.* not only indicate unusually high physisorption energies, but also strong dependence on temperature.[24] This is attributed by the authors to the following. (a) Thermal fluctuations cause large transient distortions of the C–C–C bond angles from their $T=0$ value, which is further aggravated by the frequent collisions between the H_2 molecules and the wall. (b) Deviation from planarity alters the hybridization state of carbon atom from sp^2 to sp^3, causing transient charge localization on carbon atoms. (c) Charge transfer occurs between carbon atoms and H_2 molecules nearby (donation of electrons to the antibonding states of H_2), which greatly enhances the physisorption energies.

In order to verify the above-mentioned mechanism, we carry out a three-step calculation. First, we compute the physisorption energy of one H_2 molecule on a (7,7) SWNT at $T=0$, accounting for full atomic relaxations (both the carbon and hydrogen atoms). The tetragonal supercell under periodic boundary condition is chosen to be $15.66\times15.66\times4.919$ Å in dimension, containing two (7,7) SWNT unit cells in the z direction (56 carbon atoms in all) so there is negligible interaction between a H_2 molecule and its image.[17] Second, we perform finite-temperature molecular dynamics simulation of pure SWNT at $T=300$ K—not using VASP—but using the Brenner bond-order potential with van der Waals and dihedral rotation interactions,[26] to map out the C–C–C angle distribution, in order to check with Ref. 24 Our rationale is that even though the Brenner potential is not highly accurate, it does yield approximately the right moduli and vibrational spectra of SWNTs, so it should give roughly the right angular fluctuation distribution. Lastly, we randomly take a set of configurations from the molecular dynamics trajectory obtained earlier, and calculate the total energy with or without the H_2 molecule (here, we fix the carbon atoms and only relax the hydrogen atoms). The difference in total energies is defined to be the "instantaneous" Δh, which will be averaged and then compared with Ref. 24. Our density functional theory calculations are all performed using VASP v4.4.5,[25] with the electron exchange and correlation functional being that of Ceperley and Alder[27] as parametrized by Perdew and Zunger.[28] The ultrasoft pseudopotentials for carbon and hydrogen in the VASP library[25] are used. The plane wave energy cutoff is 358 eV and charged density is expanded to 550 eV. The **k**-space sampling is performed with the method of Monkhorst and Pack[29] using $1\times1\times26$ grid. Static relaxation of ions stops only when the change in total energy is less than 1 meV. Because we are subtracting off large energies to get the adsorption energy which is tiny, this setup (supercell size, energy cutoff, **k**-space sampling, etc.) remains unchanged even for the isolated H_2 molecule calculation. For ease of verification, our input files and results are put at a publicly available web site.[30]

Before moving on, we recognize that our "instantaneous" Δh (thermally averaged) is not the same as the Δh in Ref. 24. However, if the reason for the abnormal physisorption energy is the distortion of the C–C–C angles as stated by Cheng *et al.*, then it will also manifest in our results, especially if the magnitude of the angular distortion is roughly the same. The reason that we choose a slightly different setup to compare with Ref. 24 is because we are concerned with the accuracy of our results. We simply could not afford to perform thermal averaging of dynamical trajectories of 108 carbon atoms plus hydrogen to the accuracy we want, which is on the order of tens of millielectron volts.

In the first step, we find that an isolated H_2 molecule has an equilibrium bond length of 0.768 Å, and the isolated SWNT has an equilibrium C–C bond length of 1.415 Å, in good agreement with reference results. The endohedral physisorption energy is computed to be 0.114 eV/H_2 or 2.63 kcal/mol after full atomic relaxations (56 carbon plus 2 hydrogen atoms). This is much smaller than what is reported for Δh in Ref. 24, but because it is a zero-temperature result, there is yet no contradiction. We note that this level of physisorption binding obtained from first-principles can explain the large hydrogen uptake at liquid nitrogen temperature as measured by Ye *et al.*[21]

In the second step, we perform molecular dynamics simulations of various SWNT configurations at $T=300$ and 600 K using the Brenner potential.[26] The qualitative description in Ref. 24 that rather large angular distortions exist at $T=300$ K has been verified, although we also find significant system-size dependence at small number of unit cells. Figure 2 shows the distribution of longitudinal angles (angle formed by three consecutively translated atoms in the longitudinal direction) for a (9,9) SWNT at $T=300$ and 600 K. In addition to longitudinal angle fluctuation, there is also significant radial angle fluctuation. Figure 3(a) shows the cross-sectional view of a typical (9,9) SWNT configuration during the simulation at $T=300$ K.

Despite the agreement mentioned, we also see some important differences with Ref. 24, viz. (a) our results suggest the angular distribution is a smooth function without shoulders or cusps, and (b) the contrast between $T=300$ and 600 K results is larger in Ref. 24 than in Fig. 2. If (a) is true, then the odd-shaped distribution in Ref. 24 must be either due to (1) insufficient statistics, or (2) the energy model has artifacts because of DFT accuracy/convergence issues. For reasons of either (1) or (2), the final statistically averaged Δh result would be negatively influenced, when (a) is in fact correct.

We then use the same program to generate (7,7) SWNT configurations at $T=300$ K. Because these configurations are to be later used in DFT calculations, their longitudinal dimensions have to be small (in fact, just two unit cells). This suppresses the longitudinal angle fluctuation, but the radial angle fluctuation appears to be affected little. Figure 3(b) shows the cross-sectional view of a typical (7,7) nanotube configuration during the molecular dynamics simulation at $T=300$ K. We will use this configuration to illustrate the third-step calculation.

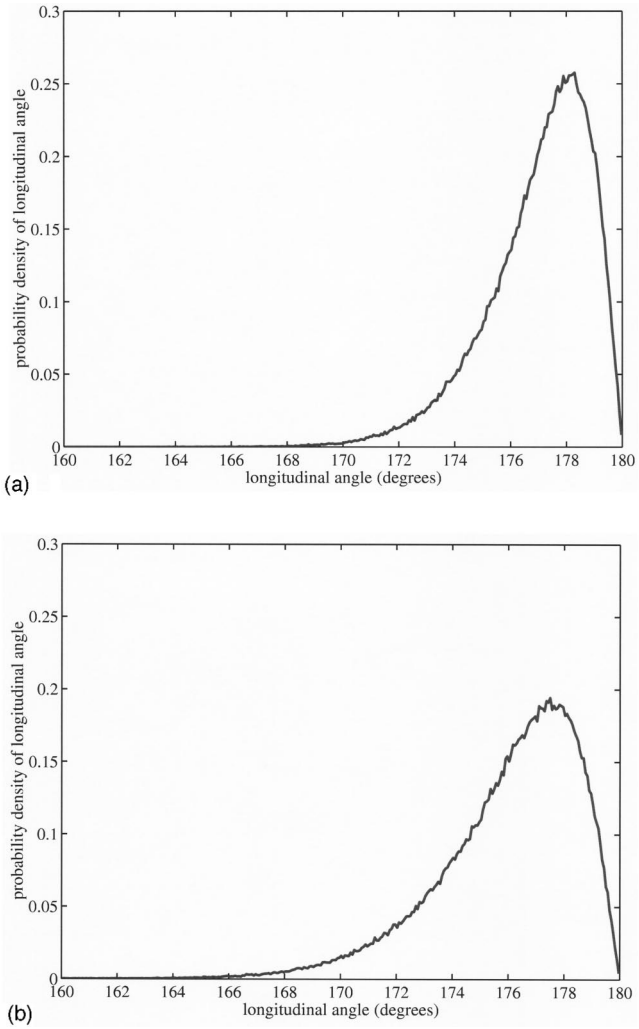

FIG. 2. Distribution of longitudinal angles (angle formed by three consecutively translated atoms in the longitudinal direction) for a (9,9) SWNT at (a) $T=300$ K and (b) $T=600$ K, obtained using the Brenner potential (Ref. 26). The molecular dynamics simulation contains ten SWNT unit cells to eliminate system-size dependence.

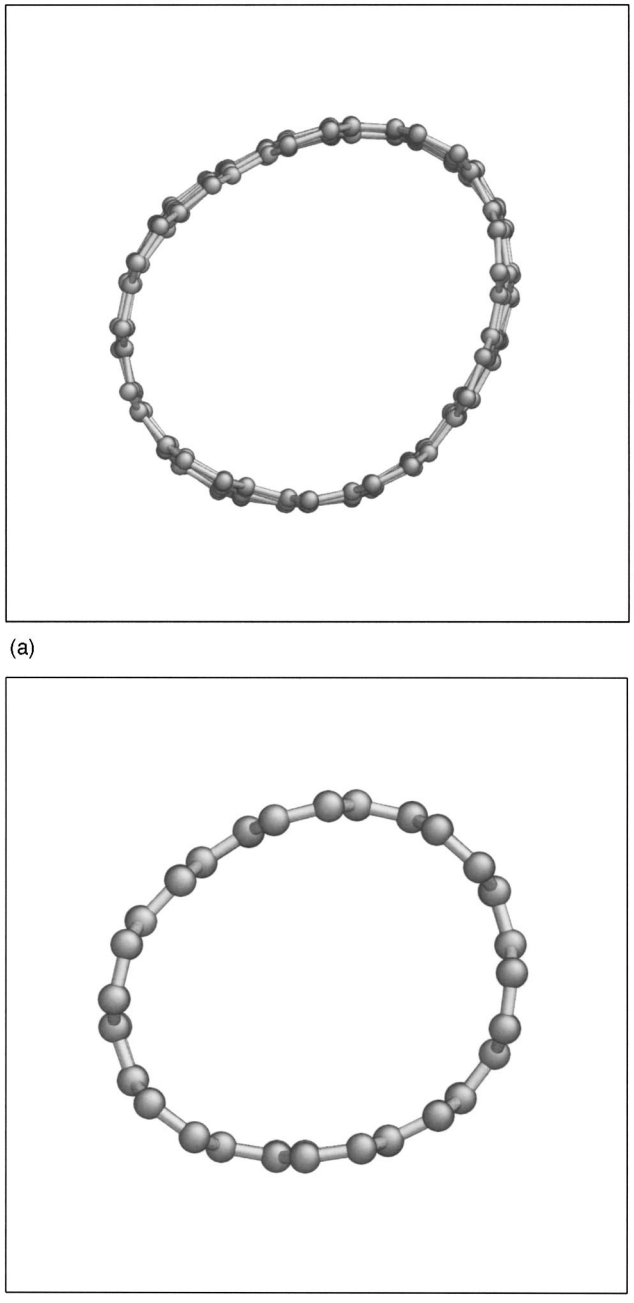

FIG. 3. Typical cross-sectional view of (a) (9,9) SWNT, and (b) (7,7) SWNT, at $T=300$ K.

In the third-step, we randomly select a set of (7,7) SWNT configurations from the above mentioned molecular dynamics trajectory. For each configuration, we first compute its total energy using VASP[25] without any relaxation, then place one H_2 molecule at different positions nearby, and perform static relaxations on just the H_2 molecule. The difference in total energies accounting for isolated H_2 molecule energy is defined to be the instantaneous adsorption energy ΔE. Our objective is not to obtain an accurate average of ΔE, but rather to check if it has the same magnitude as reported in Ref. 24 near a nanotube distorted by thermal fluctuation at $T=300$ K. A set of our results is shown in Fig. 4, along with the final configuration in which the H_2 molecule is locally relaxed to 1 meV in total energy.

We find no discernible increase in the adsorption energy in the vicinity of a distorted nanotube, as shown in Fig. 4, compared to the $T=0$ result obtained by full relaxations, which is $\Delta E=0.11$ eV/H_2 or 2.6 kcal/mol H_2. On the contrary, our results indicate the adsorption energy may decrease significantly. From our data set, we also do not find definite correlations between locally acute C–C–C angles and larger instantaneous adsorption energies. In terms of statistics, none of our configurations yield instantaneous adsorption energies greater than 2.6 kcal/mol, with an average at about 1.8 kcal/mol, which differs appreciably from the 7.51 kcal/mol endohedral physisorption enthalpy reported in Ref. 24.

In summary, from our limited calculations we have not found abnormal interaction between H_2 and the nanotube that is outside the range of ordinary van der Waals interactions between a H_2 molecule and a flat graphene sheet or graphite surface.[16,18,19] Our results seem to support various experiments[6,21,22] which suggest that high-capacity hydrogen storage (>6 wt%) can only be achieved at liquid nitrogen

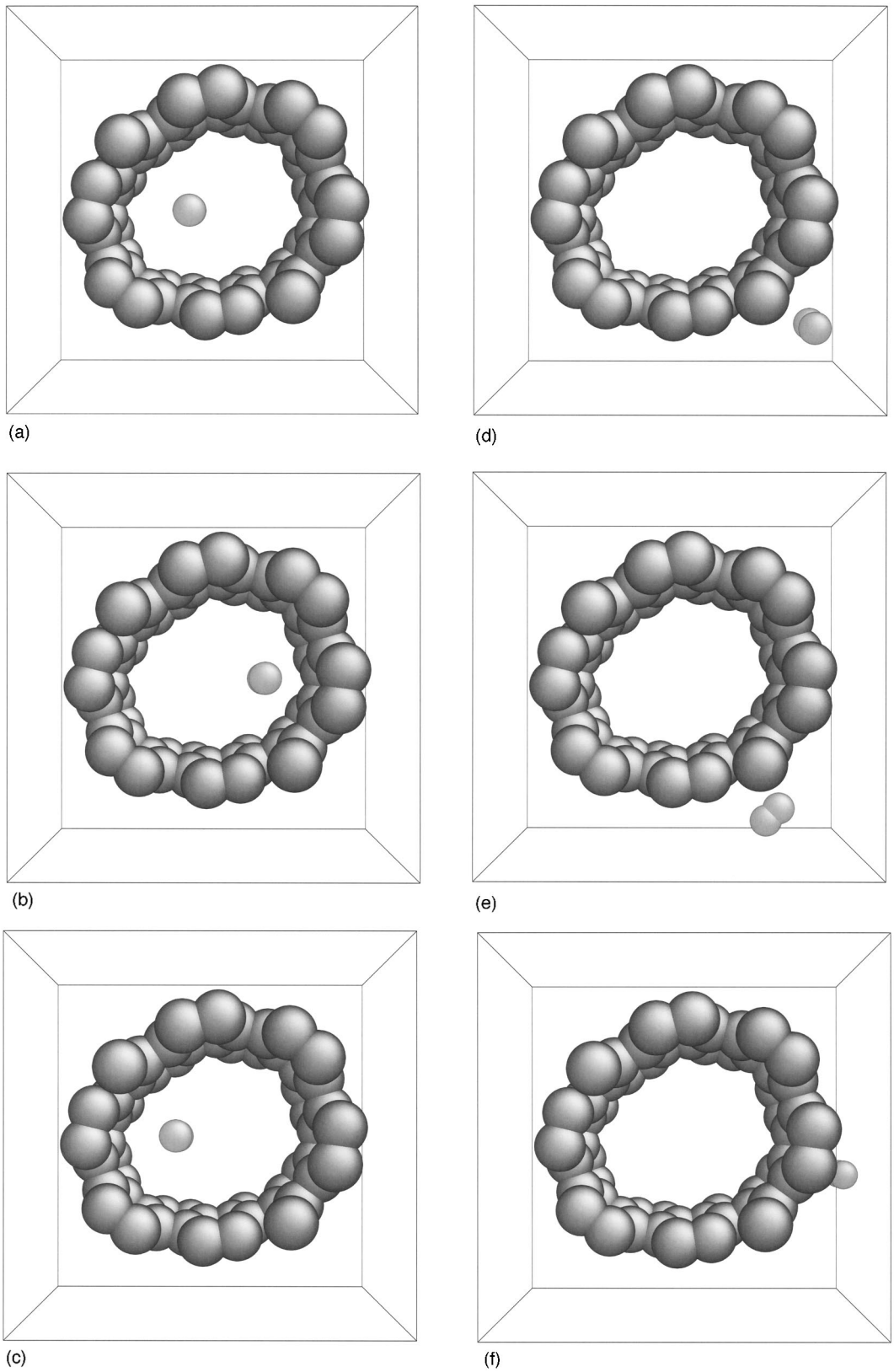

FIG. 4. Various partially stable configurations (outcome of relaxing H_2) with the corresponding adsorption energies (a) $\Delta E = 1.25$ kcal/mol, (b) $\Delta E = 2.63$ kcal/mol, (c) $\Delta E = 1.84$ kcal/mol, (d) $\Delta E = 1.30$ kcal/mol, (e) $\Delta E = 1.55$ kcal/mol, (f) $\Delta E = 2.53$ kcal/mol. The nanotube configuration is that of Fig. 3(b).

temperatures, but not at near room temperatures in pure carbon nanostructures. In contrast, the calculations of Cheng *et al.* seem to provide support for the other experiments.[1,4] Noting the difficulty of the calculations and also the inherent problem of DFT in accounting for the van der Waals interactions, we strongly encourage other researchers to perform more *ab initio* calculations to resolve this issue.

If one excludes physisorption as a significant absorption mechanism at room temperature, then we need either chemisorption (in the conventional sense) with possibly help from metal catalysts to accelerate the adsorption/desorption kinetics, or a new mechanism that is yet to be elucidated.[7] Section IV is devoted to chemisorption.

IV. DENSITY FUNCTIONAL THEORY CALCULATION OF CHEMISORPTION ENERGIES

In contrast to physisorption, which theoretically is unbounded in its hydrogen uptake, we regard 7.7 wt % as a plausible upper-bound on the chemisorption capacity in predominantly sp^2-character carbon nanostructures, which include single- and multiwalled nanotubes, fullerenes, and graphitic nanofibers. 7.7 wt % corresponds to one-to-one hydrogen to carbon ratio, where every hydrogen atom forms a direct heteronuclear bond with one carbon atom which was sp^2-hybridized originally, but is converted to sp^3-hybridized during the process.

Using density functional theory, we have examined three possible chemisorption configurations at full coverage (see Fig. 5) following similar setups to Refs. 12 and 13: inside, outside, and zigzag, which refers to the positions of the hydrogen atoms with respect to the SWNT, among which the zigzag configuration is expected to be the global energy minimum due to its structural compatibility with the sp^3-hybridization scheme. Our calculations, to be detailed later, indicate that the inside configuration is unstable and the hydrogen atoms would spontaneously break off from the SWNT wall to pair and form H_2 molecules. The outside configuration is metastable, but has a *larger* total energy compared to the reference system of isolated (7,7) SWNT and H_2's, and is therefore unrealistic. The zigzag configuration is found to be stable, having a nontrivial chemisorption energy of 0.36 eV/H with respect to the above-mentioned reference system. This binding energy may in fact be too large for room-temperature applications. As shown in Sec. II, we expect $\Delta h(X)$ to range from 0.15 eV/H to 0.2 eV/H in order to have absorption/desorption peak between $T=300$ and 400 K. Since $\Delta h(X)$ usually decreases monotonically with increasing X, our result of 0.36 eV/H for the average binding energy indicates that desorption would likely to occur only at $T>600$ K, which would be too high for vehicle applications.

Parallel to the thermodynamics considerations, there are the kinetics considerations. For practical use, we would like both the adsorption and desorption of hydrogen to happen on the time scale of seconds, thus $\nu e^{-\Delta E/k_B T}\sim 1\ \mathrm{s}^{-1}$. With the trial frequency ν taken to be on the order of $10^{13}\ \mathrm{s}^{-1}$, which is the Debye frequency of the SWNT, the activation energy ΔE is required to be ~ 0.7 eV for room temperature operations. This is less of concern for physisorption, because as

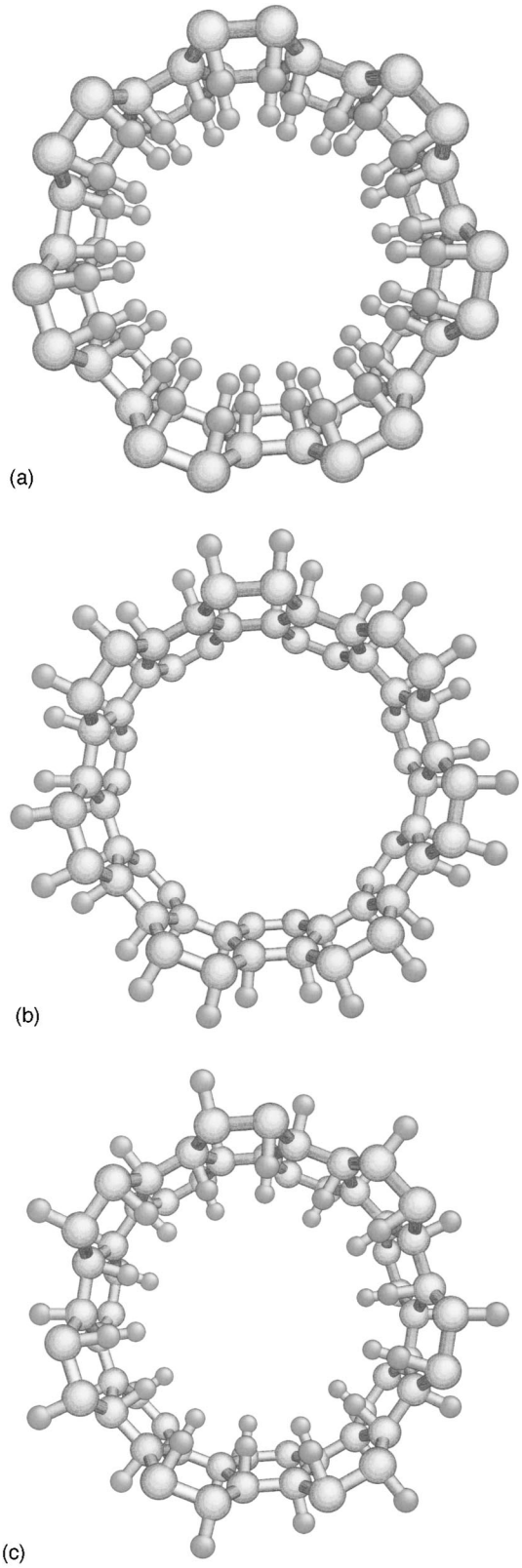

FIG. 5. Initial configurations for studying chemisorption on (7,7) SWNT: (a) inside, (b) outside, (c) zigzag. The initial C–H bond lengths are all 1.1 Å.

Arellano *et al.*[16] have shown, the energy barrier of the H_2 molecule translating on the graphene sheet is quite small compared to the binding energy, and is therefore likely to be smaller than 0.7 eV. Steric factors such as nanotube termina-

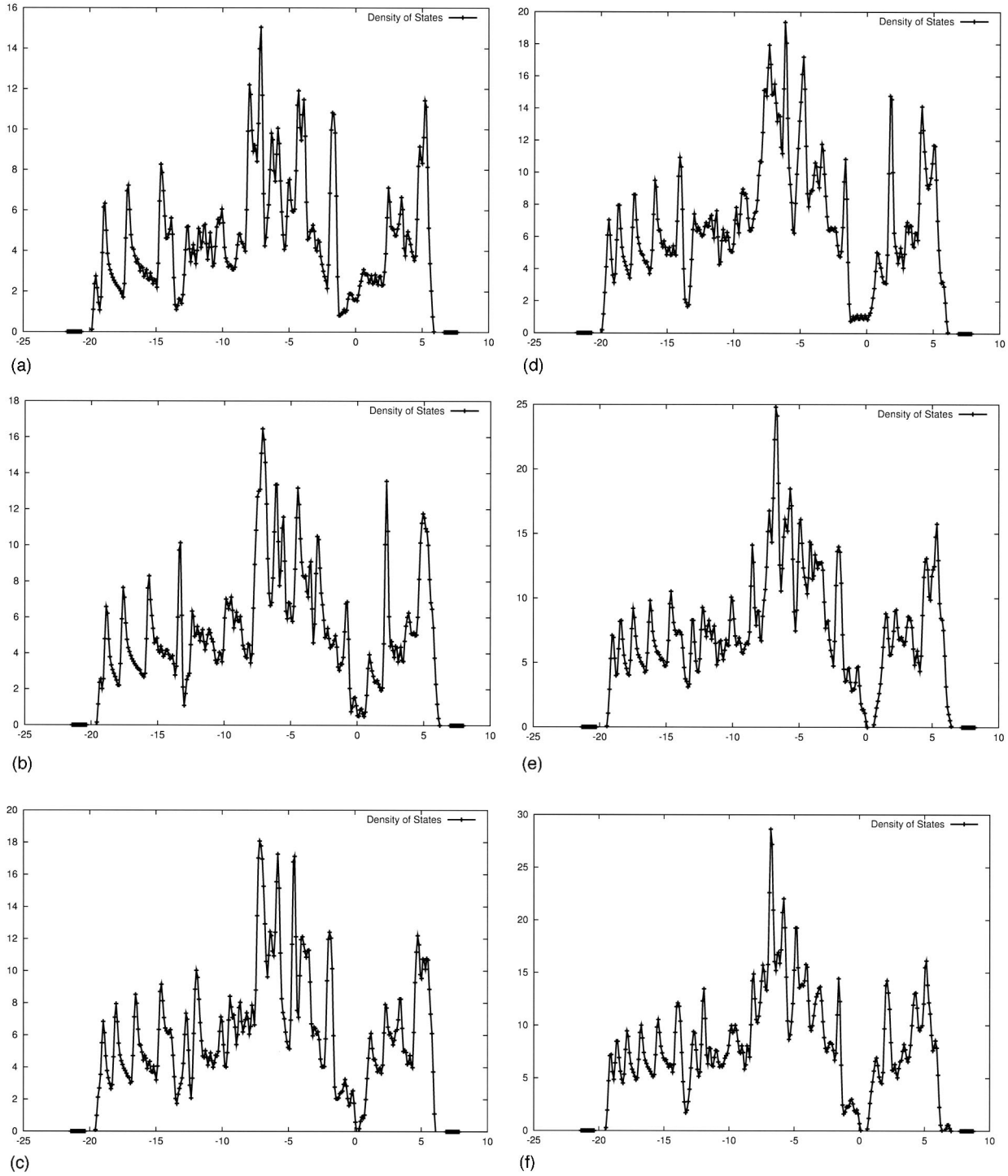

FIG. 6. Calculated electron DOS of isolated relaxed zigzag nanotubes. (a) (6,0) SWNT, (b) (7,0) SWNT, (c) (8,0) SWNT, (d) (9,0) SWNT, (e) (10,0) SWNT, (f) (11,0) SWNT. The DOS have been shifted so the Fermi levels are at zero.

tion condition and length-to-diameter ratio can be controlled, for example, by ultrasonic cutting. The activation energy however could be a fundamental problem for the *chemisorption* kinetics of hydrogen in carbon nanostructures, since the binding energy of H_2 molecule is 4.7 eV, and the H–H bond certainly needs to be broken in order for chemisorption to occur. Work in the literature has been reviewed in Ref. 14. In the following we would like to make some remarks from a bonding perspective.

We think that in order for fast adsorption/desorption of hydrogen to occur at room temperature, some bonding or interaction of *metallic* nature is required. Such interactions may of course be introduced by metal-catalyst particles nearby, such as Pd, Pt, and Rh, but this subject would be too

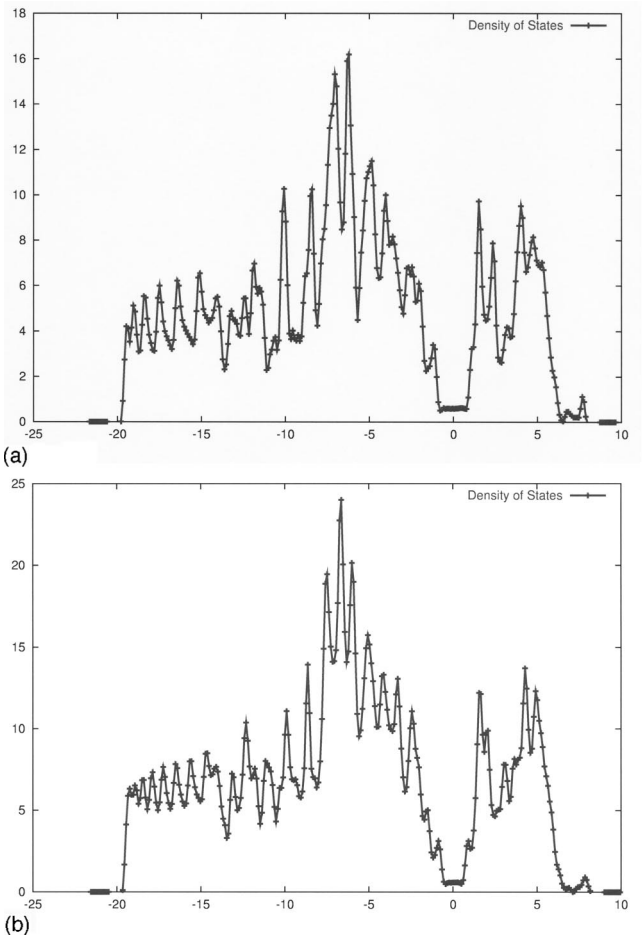

FIG. 7. Calculated electron DOS of isolated relaxed armchair nanotubes. (a) (7,7) SWNT, (b) (10,10) SWNT. The DOS have been shifted so the Fermi levels are at zero.

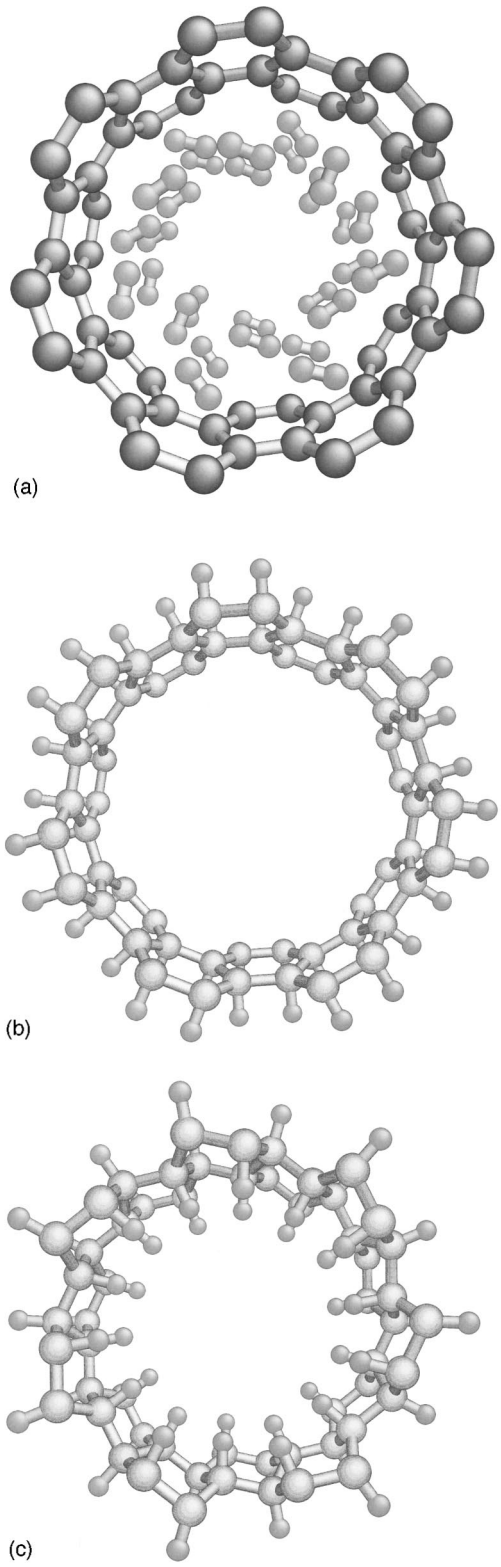

FIG. 8. Relaxed configurations of hydrogen chemisorption on (7,7) SWNT: (a) inside, (b) outside, (c) zigzag, starting from the initial configurations shown in Fig. 5.

complicated for discussion now. Here what we would like to focus on is the intrinsic metallicity of some carbon nanotubes and how it is influenced by the introduction of hydrogen, from which we can obtain some general understanding about the chemical environment.

We perform density functional theory calculations of SWNTs before and after hydrogen chemisorption using VASP under the same set of conditions as those specified in Sec. III, except the supercell now contains one SWNT unit instead of two, and the **k**-point sampling uses $1\times1\times56$ grid instead of $1\times1\times26$. Static relaxations have been carried out on isolated $(n,0)$ (''zigzag'') nanotubes ranging from (6,0) to (11,0), and on isolated (n,n) (''armchair'') nanotubes (7,7) and (10,10). The electron densities of states (DOS) of the relaxed configurations are shown in Figs. 7 and 8, respectively. Using a simple tight-binding model,[31] one can show that all armchair nanotubes are metallic; among the zigzag nanotubes, the $(3n,0)$ type is metallic, while the $(3n+1,0)$ and $(3n+2,0)$ types are semiconducting. As can be seen in Figs. 6 and 7, the theoretical predictions are correct except for the (7,0) SWNT, which might be due to a small radius effect. All our input files and results are placed at a publicly available web site.[30]

However, a recent experiment[32] using scanning tunneling microscopy indicates that even the $(3n,0)$ type zigzag nanotubes may have gaps in the measured DOS. It is known that a band gap could open up in a metallic SWNT once it is no longer isolated and comes into contact with impurities or other nanotubes. Since our results are based on a general method in a strictly controlled setup, we feel the measure-

ment results could arise from finite tube length or contact effects instead of intrinsic behavior of $(3n,0)$ nanotubes.

Metallicity separates carbon nanotubes, at least some types of it, from other pure carbon nanostructures, and is the fundamental reason for unique chemical and transport properties (the same can also be said for conducting polymers). The existence of delocalized electrons is a consequence of the ring-resonance and long-range order of the nanotube, and could be fragile with respect to perturbations or impurities. We are tempted to postulate that once the metallicity of a carbon nanotube is lost completely, its chemical properties so far as binding and reaction-activation energetics with hydrogen are concerned can no longer be very distinct from other sp^2-dominated carbon nanostructures.

Going back to the calculations, we have relaxed the three initial configurations shown in Fig. 5 under the same conditions as for the isolated SWNTs. For the inside configuration [Fig. 5(a)], it undergoes structural instability and turns into the configuration shown in Fig. 8(a), which incidentally corresponds to physisorption at very large (7.7 wt %) H_2 concentration. However, the binding energy turns out to be -1.1 eV/H_2, so the configuration would not actually exist in nature. This negative binding energy is probably due to the large H_2-H_2 repulsion. As Diep *et al.*[17] have shown, once the distance between two H_2 molecules is less than 2.5 Å, strong intermolecular repulsion will occur.

For the outside configuration [Fig. 8(b)], we find the nanotube undergoes significant radial expansion: the tube diameter actually increases from 9.5 to 11.1 Å, by about 17%. The C–H bond distance turns out to be 1.094 Å, which does not differ much from those of hydrocarbons (1.10 Å in methane). This radial expansion can be attributed to the increased coordination number of carbon, which weakens the original bonds. For comparison, there is about 8.5% bond length increase associated with going from graphite to diamond. The chemisorption energy is -0.68 eV/H. So again, this is an unrealistic configuration. However, it is still interesting to see what happens to the electron DOS which we know is metallic for the isolated (7,7) SWNT [Fig. 7(a)] when the hydrogen atoms are not yet chemisorbed. Figure 9(a) shows that a narrow band gap of ~ 0.8 eV has opened up after the hydrogen atoms are chemisorbed on the outside.

For the zigzag configuration, the inside C–H bond length turns out to be 1.118 Å and the outside C–H bond length turns out to be 1.110 Å, respectively. The nanotube itself undergoes a puckering transformation where one atom in the unit cell expands outward (outer tube diameter increases from 9.5 to 10.3 Å by about 8.4%), and another atom in the unit cell shrinks inward (inner tube diameter decreases from 9.5 to 9.4 Å by about 1.0%). Remarkably, the reconstructed C–C bond lengths are 1.53 and 1.50 Å (from the starting 1.410 and 1.415 Å), which are rather close to the C–C bond length of 1.54 Å in diamond (1.42 Å in graphite). The C–C–C bond angles change from 120° to 106° and 110°, and the H–C–C bond angles change from 90° to 111° and 112°, respectively, which are also quite close to the ideal tetrahedral angle of 109°. This verifies the picture of transition from sp^2- to sp^3-bond types when the hydrogen atoms are chemisorbed.

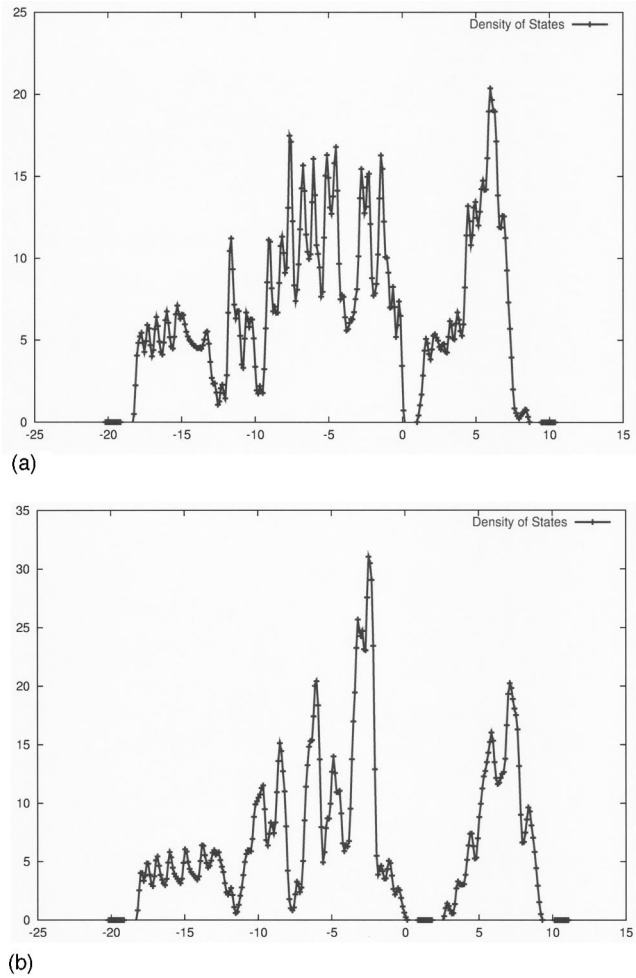

FIG. 9. Calculated electron DOS of relaxed (a) outside [Fig. 8(b)], and (b) zigzag [Fig. 8(c)] H-chemisorption on (7,7) SWNT configurations. Compared to Fig. 7(a), a narrow band gap of ~ 0.8 eV is seen to open up in (a), and a wider band gap of ~ 2.5 eV in (b).

What happens to the electron DOS? From Fig. 9(b), we see that a rather large band gap of ~ 2.5 eV has opened up in the originally conducting DOS [compare with Fig. 7(a)]. This indicates that at the maximum coverage, the bonding environment has turned fully covalent. This is not good news for the kinetics because activation energies tend to be much greater in covalently bonded environments than in metallic environments. At the very least, in the hydrogen desorption stage, strong covalent C–H bonding would slow down the kinetics of H_2 recombination. This may not be a big problem at $T > 600$ K, but certainly may be a critical problem at room temperature.

V. DISCUSSIONS

Breaking up the H_2 molecule at room temperature has been a long-standing challenge not limited to just hydrogen storage. In fuel cells, this has been achieved up to now by introducing metal catalysts. How to use the minimal amount of platinum-group metals while maintaining the catalytic efficiency is a very active field of research. It is our opinion that unless a remarkable new effect exists between hydrogen and carbon nanotube, spontaneous disassociation of H_2 near

pure carbon nanotubes is unlikely at room temperature. So we think chemisorption, though energetically favorable (still there is the problem of too strong binding, leading to only $T>600$ K desorption), may be severely hampered by slow kinetics. This problem however could be ameliorated by introducing metal catalysts and/or deformation processing,[33] where one finds that coordination-2 carbon radicals can break up the H_2 molecule without catalysts in calculations. On the other hand, we think binding between nondisassociated H_2 molecule and carbon nanotube is so weak that physisorption is only significant at cryogenic temperatures. This is not changed even if the carbon nanotube undergoes large C–C–C angular distortion due to thermal fluctuations and molecular collisions.

From our first-principles calculations that try to emphasize accuracy, we have found no indication of abnormal hydrogen–nanotube interactions of large enough magnitude, *and which is also unique to the carbon nanotube*, that would change the above-presented picture. For instance, a simple tight-binding model could describe the structure of fully hydrogenated carbon nanotube rather well, and the sp^2- to sp^3-hybridization transition is seen to be a fitting description of the chemisorption process. The metallicity of some carbon nanotubes is a remarkable effect that distinguishes them from other pure carbon nanostructures. But we find it disappears completely at full hydrogen coverage, and we think it may be sensitive to even rather small coverage. This is a direction for future study.

In summary, we believe ~ 7.7 wt % is the upper limit to hydrogen sorption in carbon nanotubes. While measurement results on this level had been reported,[1,4] the results could not be reproduced at room temperature. We believe this upper limit would be very difficult to achieve in practice. Moreover, we find no rational reason yet for carbon nanotubes to have superior hydrogen uptake capacity than other graphitic structures in terms of either binding energies or kinetics. Independent studies[34,35] seem to reach similar conclusions.

ACKNOWLEDGMENTS

This study is supported by Honda R&D Co., Ltd., Japan. J.L. and S.Y. would like to express their appreciation for the hospitality of the Fundamental Research Lab, Wako Research Center during their visits.

[1] A.C. Dillon, K.M. Jones, T.A. Bekkedahl, C.H. Kiang, D.S. Bethune, and M.J. Heben, Nature (London) **386**, 377 (1997).
[2] A. Chambers, C. Park, R.T.K. Baker, and N.M. Rodriguez, J. Phys. Chem. B **102**, 4253 (1998).
[3] P. Chen, X. Wu, J. Lin, and K.L. Tan, Science **285**, 91 (1999).
[4] M.J. Heben, A.C. Dillon, J.L. Alleman, K.E.H. Gilbert, K.M. Jones, P.A. Parilla, T. Gennett, and L. Grigorian, Materials Research Society Fall Meeting Symposium, Z10.2, 2001.
[5] M. Hirscher, M. Becher, M. Haluska *et al.*, Appl. Phys. A: Mater. Sci. Process. **72**, 129 (2001).
[6] M. Hirscher, M. Becher, M. Haluska *et al.*, J. Alloys Compd. **330–332**, 654 (2002).
[7] R. Dagani, Chem. Eng. News **80**, 25 (2002).
[8] V.V. Simonyan, P. Diep, and J.K. Johnson, J. Chem. Phys. **111**, 9778 (1999).
[9] Q. Wang and J.K. Johnson, J. Chem. Phys. **110**, 577 (1999).
[10] Q. Wang and J.K. Johnson, J. Phys. Chem. B **103**, 4809 (1999).
[11] K.A. Williams and P.C. Eklund, Chem. Phys. Lett. **320**, 352 (2000).
[12] S.M. Lee, K.H. An, Y.H. Lee, G. Seifert, and T. Frauenheim, J. Am. Chem. Soc. **123**, 5059 (2001).
[13] S.M. Lee, K.H. An, W.S. Kim, Y.H. Lee, Y.S. Park, G. Seifert, and T. Frauenheim, Synth. Met. **121**, 1189 (2001).
[14] V. Meregalli and M. Parrinello, Appl. Phys. A: Mater. Sci. Process. **72**, 143 (2001).
[15] D.V. Schroeder, *An Introduction to Thermal Physics* (Addison-Wesley, Reading, MA, 2000).
[16] J.S. Arellano, L.M. Molina, A. Rubio, and J.A. Alonso, J. Chem. Phys. **112**, 8114 (2000).
[17] P. Diep and J.K. Johnson, J. Chem. Phys. **112**, 4465 (2000); erratum, **113**, 3480 (2000).
[18] A.D. Crowell and J.S. Brown, Surf. Sci. **123**, 296 (1982).
[19] S.C. Wang, L. Senbetu, and C.-W. Woo, J. Low Temp. Phys. **41**, 611 (1980).
[20] S. Maruyama, Oyo Butsuri **71**, 323 (2002).
[21] Y. Ye, C.C. Ahn, C. Witham, B. Fultz, J. Liu, A.G. Rinzler, D. Colbert, K.A. Smith, and R.E. Smalley, Appl. Phys. Lett. **74**, 2307 (1999).
[22] C.C. Ahn, Y. Ye, B.V. Ratnakumar, C. Witham, R.C. Bowman, and B. Fultz, Appl. Phys. Lett. **73**, 3378 (1998).
[23] K.A. Williams, B.K. Pradhan, P.C. Eklund, M.K. Kostov, and M.W. Cole, Phys. Rev. Lett. **88**, 165502 (2002).
[24] H. Cheng, G.P. Pez, and A.C. Cooper, J. Am. Chem. Soc. **123**, 5845 (2001).
[25] G. Kresse and J. Hafner, Phys. Rev. B **47**, 558 (1993); G. Kresse and J. Furthmuller, *ibid.* **54**, 11169 (1996).
[26] D.W. Brenner, Phys. Status Solidi B **217**, 23 (2000). An implementation of the potential that has nonbond and dihedral rotation interactions is available at http://www.mse.ncsu.edu/CompMatSci/
[27] D. Ceperley and B.J. Alder, Phys. Rev. Lett. **45**, 566 (1980).
[28] J.P. Perdew and A. Zunger, Phys. Rev. B **23**, 5048 (1981).
[29] H.J. Monkhorst and J.D. Pack, Phys. Rev. B **13**, 5188 (1976).
[30] For ease of verification, our input files and results are put at a publicly available web site: http://alum.mit.edu/www/liju99/Papers/03/Li03c
[31] *Physical Properties of Carbon Nanotubes*, edited by R. Saito, G. Dresselhaus, and M.S. Dresselhaus (World Scientific, New York, 1998).
[32] M. Ouyang, J.-L. Huang, C.L. Cheung, and C.M. Lieber, Science **292**, 702 (2001).
[33] S. Orimo, T. Matsushima, H. Fujii, T. Fukunaga, and G. Majer, J. Appl. Phys. **90**, 1545 (2001).
[34] A. Zuttel, Ch. Nutzenadel, P. Sudan, Ph. Mauron, Ch. Emmenegger, S. Rentsch, L. Schlapbach, A. Weidenkaff, and T. Kiyobayashi, J. Alloys Compd. **330–332**, 676 (2002).
[35] L. Schlapbach and A. Zuttel, Nature (London) **414**, 353 (2001).